Submitted to Physical Review B, *June 17, 2003*

Exciton-Exciton Annihilation and the Production of Interchain Species in Conjugated Polymer Films: Comparing the Ultrafast Stimulated Emission and Photoluminescence Dynamics of MEH-PPV

Ignacio B. Martini, Alex D. Smith and Benjamin J. Schwartz*

Department of Chemistry and Biochemistry
University of California, Los Angeles
Los Angeles, CA 90095-1569 USA

*corresponding author e-mail: schwartz@chem.ucla.edu

PACS: 78.47.+p; 71.20.Rv; 78.45.+h; 78.55.Kz

Abstract: Despite the enormous versatility of conjugated polymers for use in optoelectronic devices and the correspondingly large number of research studies on their photophysics, understanding of the fundamental nature of the primary photoexcitations remains highly controversial. Part of the reason for this controversy stems from the fact that the photophysics of conjugated polymer films depend sensitively on excitation intensity, making it difficult to compare the results of different experiments such as pump-probe stimulated emission (SE) and time-resolved photoluminescence (PL), which usually are performed at excitation intensities that differ by orders of magnitude. In this paper, we present a detailed exploration of the pump-probe SE and time-resolved PL dynamics of poly(2-methoxy 5-[2′-ethylhexyloxy]-*p*-phenylene vinylene) (MEH-PPV) films under identical excitation conditions. Using an optically-triggered streak camera, we are able to simultaneously measure the PL and SE dynamics as a function of both excitation intensity and emission wavelength. Although the SE and PL dynamics of dilute MEH-PPV solutions are identical, we find that even at low excitation intensities, the PL and SE dynamics of MEH-PPV films are different, uncovering the presence of an interchain excited-

state absorbing species that has dynamics distinct from the intrachain exciton. The number of interchain absorbing species increases non-linearly with excitation intensity, suggesting that interchain species are formed both directly upon photoexcitation and as a byproduct of exciton-exciton annihilation (E-EA). A comparison of the emission dynamics of pristine and intentionally-oxidized MEH-PPV films leads us to conclude that there are multiple types of interchain species; we propose that the directly-excited interchain species are likely aggregates or excimers, while the interchain species produced by E-EA are best assigned to polaron pairs. We also find that the wavelength dependence of the SE and PL from MEH-PPV films is complex, both because energy migration leads to a dynamic red-shift of the exciton emission and because the rate of E-EA is higher for hot (blue-emitting) excitons than for thermalized (red-emitting) excitons. All the results are compared in detail to previous work, providing a means to resolve many of the apparently contradictory ideas in the literature concerning the photophysics of conjugated polymer films.

I. Introduction:

The photophysics of semiconducting polymers are of great interest due to the numerous potential optoelectronic applications for these materials. Understanding the nature of the optically prepared excited-state(s) of conjugated polymer films is vital to the development of devices such as plastic light emitting diodes (LEDs)[1,2] and solar cells.[3,4] For example, the direct photogeneration of separated charges in the excited state is beneficial for conjugated polymer-based photovoltaics but could prove detrimental to the electroluminescence efficiency of polymer-based LEDs. As a result, the photophysics of conjugated polymers[5–31] and, in particular, that of poly(2-methoxy 5-[2′-ethylhexyloxy]-*p*-phenylene vinylene) (MEH-PPV),[32–52] have been the subject of intense study. Despite all this effort, the answers to many fundamental questions remain controversial, including: the degree of charge separation in the initially-prepared excited state and the role and origin of possible interchain electronic species.

Answering these questions is challenging for several reasons. First, there are multiple ways in which excited neighboring conjugated polymer chromophores can interact, leading to the possibility of interchain electronic species with differing degrees of charge separation.[45] Second, interchain species might form in either the ground or electronic excited states, leading to the possibility that interchain species could be excited directly as well as populated via energy transfer from ordinary single-chain excitons;[35] Third, the formation of interchain species and the degree of charge separation are likely to be affected by the intensity of the excitation light used to study the conjugated polymer.[10] In particular, neighboring excitons at high excitation densities can interact via Auger processes, leading to non-radiative mechanisms for the destruction of excitons that do not exist at low excitation intensities. We refer to this type of process as “bimolecular recombination” or “exciton-exciton annihilation” (E-EA).[6] In what

follows we will refer to two conjugated segments that share their π electrons equally in the excited state as "excimers",[15–17,39,53] and to adjacent segments with charge transfer character (i.e. a hole on one segment Coulombically bound to an electron on a neighboring segment) as "polaron pairs" or "spatially indirect excitons".[32–37] Interchain species in which the π–conjugated electrons are delocalized in the ground state will be called "aggregates".[22–26,43,44]

A. Controversy over Interchain Species in Conjugated Polymers: With all the different possibilities for interchain species and their dependence on excitation intensity, it is not surprising that different results in the literature point to different and often conflicting conclusions. For example, McBranch and co-workers, who studied the photophysics of an oligomer of MEH-PPV, have argued that interchain species are formed in semiconducting polymers only at high excitation intensities.[10–12] In other words, McBranch and co-workers believe that interchain species either form only as a byproduct of E-EA or are created directly from doubly-excited excitons. Similar conclusions have been offered by Denton *et al.*[8] and Stevens *et al.*[9] based on intensity- and wavelength-dependent studies of the photophysics of unsubstituted PPV and polyfluorene derivatives, respectively. In contrast, Rothberg and co-workers, who studied both MEH-PPV solutions and films, believe that a large fraction (≥ 50%) of very weakly-emissive interchain species are produced directly upon excitation, even at very low excitation intensities.[32–39] Rothberg and co-workers have alternately assigned the interchain species both as excimers[39] and polaron pairs,[32–37] and have been able to explain the photophysics they observe with a simple two-species model.[36,37] A related conclusion concerning the direct production of polarons has been reached by Heeger and co-workers, whose investigations of the absorption of infrared-active vibrations (IRAV) in MEH-PPV films suggest that at least 10% of the excitations result in the direct production of separated charges.[50,51] We have summarized

many of the details of the controversy over interchain species in semiconducting polymers in recent reviews.[45,46]

In an effort to reconcile many of the conflicting results, we previously performed a series of studies investigating the photophysics of MEH-PPV[44–48] and related conjugated polymers[30,31] as a function of the conformation of the polymer chains. We found that under conditions where the polymer coils interpenetrate, conjugated polymer solutions show the spectral signatures (weak red shifted absorption and emission) of the formation of ground state interchain aggregates.[31,44] Thus, solutions with increased chain interpenetration (e.g. solutions with high concentrations of polymers that form relatively open coils[44] or solutions in which the chains are driven together by the addition of non-solvents[17,23,36,37]) show increased chromophore aggregation, while solutions with poorer chain overlap (e.g. solutions of polymers in poor solvents with tight chain coils or solutions of conjugated ionomers in which the chain coils have been collapsed[31]) show little chromophore aggregation. We also have argued that the degree of chromophore aggregation in solution survives the spin-coating process and persists into the film,[45,46] a result consistent with more recent studies of single MEH-PPV molecules.[54–56] Thus, conjugated polymer films cast from solutions with different solvents or different polymer concentrations have different degrees of interchain interaction. Differences in the degree of interchain interaction in conjugated polymer films with different processing histories, in turn, lead to different photophysical and electrical properties, including: changes in exciton lifetime and emission quantum efficiency,[28,46] variations in carrier mobility,[57,58] alterations of the ability of the films to undergo lasing or amplified spontaneous emission,[59–61] and modification of the degree to which E-EA can occur at high excitation intensities.[27,30,46] This sensitivity to film morphology can explain much of the controversy over the photophysics of conjugated polymer

films, since different research groups tend to process their polymer films in different ways, so that different groups have studied films with different degrees of interchain interaction.[45,46]

Although differences in film morphology can explain much of the controversy in the literature, there are still several fundamental questions concerning the electronic structure of conjugated polymers that remain to be answered. For example, what are the excited-state spectral manifestations of interchain species? Do interchain species exist at low excitation intensities, or are high intensities required for their creation? What is the connection between E-EA and the existence of interchain species? In this paper, we will address these questions by performing a detailed study of the photoluminescence (PL) and stimulated emission (SE) dynamics of MEH-PPV films under identical experimental conditions. The results allow us to uncover the presence of an interchain electronic absorption in the region where the polymer emits and to investigate the behavior of this absorption as a function of excitation intensity. We find that interchain species are created both directly upon excitation and as a byproduct of E-EA, providing a means to tie together many of the open questions in the literature.

B. Basic Features of Conjugated Polymer Photophysics: To place our results in context, we first briefly review the nature of the photophysics of conjugated polymers, focusing our attention on MEH-PPV. The simplest (and least controversial) place to begin is with an examination of the behavior of isolated conjugated polymer chains in dilute solution. It is generally accepted that the electronic structure of isolated conjugated polymer chains in dilute solution is dominated by singlet intrachain excitons. In ultrafast pump-probe experiments, the presence of excitons can be monitored both by SE, at wavelengths in the visible where the exciton luminescences, and by photoinduced absorption (PA), via an excited-state absorption band. For MEH-PPV, the singlet exciton PA occurs in the near infrared, peaking near 800 nm.[32,33,49] Excitons also can be

monitored through their emission dynamics via time-correlated single photon counting (TCSPC)[6,16,39] or fluourescence upconversion.[18,41] If the chromophores are isolated in dilute solution, then there should be minimal formation of interchain species,[26,35] leading to the expectation of identical relaxation dynamics for the SE, PA, and PL, each of which simply reflect the excited-state lifetime of the exciton.

Figure 1 compares the decay dynamics of the SE monitored at 580 nm (open symbols) and the spectrally-integrated PL (solid and dashed curves) at two pump intensities that differ by over an order of magnitude for a dilute solution of MEH-PPV in chlorobenzene. When the instrument response is taken into account (see section II below),[62] each of the four traces in Fig. 1 fit well to a single exponential decay with a 315-ps time constant, in agreement with previously published data for this system.[35,44,49] The identical kinetics observed in all four traces confirm the picture that only a single excited-state species, the singlet exciton, is present when the chains are isolated in dilute solution. This finding is consistent with the conclusions reached in studies of a variety of semiconducting polymer systems by several groups.[16,25,35,44,49]

In addition to the simple decay kinetics, the absence of any intensity-dependence to the emission dynamics in Figure 1 shows that E-EA does not occur when the MEH-PPV chromophores are isolated in solution. This makes sense in light of the fact that exciton diffusion along the backbone of a conjugated polymer chain is much slower than Förster energy transfer between chains:[63,64] excitons simply cannot diffuse far enough during their lifetime, so they have difficulty finding each other to annihilate when the chains are isolated. In fact, the intensity independence extends over a much larger range than indicated in Figure 1: the PL dynamics of dilute solutions of conjugated polymers measured with TCSPC or upconversion agree well with those measured in pump-probe SE experiments, even though the excitation

intensities in pump-probe experiments are typically more than two orders of magnitude higher than those used to measure the PL dynamics.

In contrast to the simple photophysical behavior in dilute solution, the photophysics of conjugated polymer films are strongly dependent on excitation intensity. Figure 2A shows the spectrally-integrated PL decay that results from excitation of an MEH-PPV film spin-cast from chlorobenzene at three different pump fluences. The PL decay is clearly intensity dependent, with the initial part of the decay becoming faster at higher excitation intensities. This type of intensity-dependent change in the emission dynamics is the classic signature of E-EA, and has been observed by many groups in a wide variety of semiconducting polymer systems.[6–13,27,31,46] At early times, the concentration of excitons is the highest, and the close proximity of neighboring excitons in the film allows for rapid E-EA. As the nearby excitons annihilate and it becomes increasingly difficult for the remaining excitons to encounter one another, the exciton decay rate approaches that of isolated excitons created at low excitation densities.

In addition to the strong sensitivity to excitation intensity, the photophysics of conjugated polymer films (but not solutions) are also highly dependent on detection wavelength. Figure 2B shows spectrally selected PL dynamics from the same MEH-PPV film studied in Fig. 2A, collecting only the red (dashed curve) or blue (solid curve) portions of the emission spectrum (*cf.* Fig. 3, below). The data indicate clearly that the PL dynamics depend on wavelength, with the blue portion of the emission showing a much faster decay at early times than the red portion of the emission. This results from the close contact between the polymer chains in the film environment that allows for rapid (Förster) energy migration from higher energy to lower energy sites. The rapid energy transfer gives rise to spectral diffusion that results in a faster initial decay

of the higher-energy portion of the fluorescence spectrum, as also has been observed by several groups.[18–21,41,42]

The final difference between the photophysics of conjugated polymers in solutions and films is evident in the fact that conjugated polymers have much lower PL quantum yields in films than in solution. This could result either from exciton-exciton annihilation, which non-radiatively lowers the population of excitons at early times in films but not in solution, or from the existence of poorly emissive interchain species, which occur only in films. For all the possible types of interchain species--aggregates, excimers or polaron pairs--the delocalization of electron density between chains leads to the expectation of a red-shifted emission with extremely low quantum yield.[14,16,22,39,45,53] Thus, conjugated polymer films have lower PL quantum yields than conjugated polymer solutions either because a significant fraction of the directly-excited species are interchain, or because a significant fraction of the emissive excitons migrate to lower-energy interchain sites.

C. The Spectral Signatures of Interchain Species in Conjugated Polymer Films: In addition to their low emission quantum yield, interchain species in conjugated polymer films also are characterized by a distinct excited-state absorption, or interchain PA. Thus, in principle, it should be possible to distinguish the dynamics of the intra- and interchain species by separately monitoring the emission dynamics of the intrachain exciton and the PA of the interchain species. Unfortunately, the interchain PA nearly always occurs to the red of the polymer's ground state absorption spectrum, where it overlaps with both the exciton emission and exciton PA bands.[10–12] This leads to spectral congestion that makes it difficult to sort out the contributions from intra- and interchain species in pump-probe SE or PA experiments. Alternatively, one could monitor the intrachain exciton dynamics using time-resolved PL, but the excitation intensities used to

measure PL via upconversion or TCSPC are so much lower than those used to measure PA in pump-probe experiments that there is no simple way to account for differences in dynamics due to E-EA, let alone the possible intensity-dependent production of interchain species.

Clearly, to unravel the photophysics of interchain species in conjugated polymer films, it is important to measure both emission and absorption dynamics at the same excitation intensities. In particular, it is constructive to measure the PL and pump-probe dynamics at the same wavelengths and excitation intensities. This is because the pump-probe signal in the emission region consists of a sum of SE gain from the intrachain exciton and excited-state absorption from any interchain electronic species. If the dynamics of the emissive excitons are also monitored via PL, then the difference between the PL and SE signals contains direct information about the dynamics of the interchain PA. In other words, if the PL and SE decays are identical, as in Figure 1, then only intrachain excitons are present following excitation. However, if the PL and SE decays do not agree, then the difference between them must be a direct reflection of the presence of an interchain PA whose dynamics are distinct from those of the emissive intrachain exciton.

In this paper, we perform a detailed investigation of the PL and SE dynamics of MEH-PPV films. By taking advantage of an optically-triggered streak camera, we are able to simultaneously measure the PL and SE dynamics, so that the excitation intensity and geometry are identical for both measurements. We then explore the PL and SE dynamics of MEH-PPV films as a function of both excitation intensity and detection wavelength. We find that even at very low excitation intensities the PL and SE measurements show significantly different decay dynamics, indicating that interchain species with distinct PA dynamics in the emission region do exist in conjugated polymer films. The magnitude of the interchain PA increases non-linearly

with excitation intensity, suggesting that interchain species can be formed both directly upon excitation and as a byproduct of E-EA. Moreover, we also measure SE and PL at different spectral positions, and find a noticeable wavelength dependence to the decay dynamics. This result implies that the photophysics of conjugated polymer films in the visible part of the spectrum are characterized by an intricate competition between many processes, including: a dynamic spectral shift of the interchain PA, wavelength-dependent E-EA, intensity-dependent production of interchain species, and exciton migration through an inhomogeneous density of states. Thus, we conclude that no simple single dynamical picture can describe the photophysics of conjugated polymer films.

II. Experimental Setup

The time-resolved SE experiments presented in this paper were performed with a femtosecond laser system that has been described previously.[46] Briefly, the laser system consists of a regeneratively-amplified Ti:Sapphire laser (Spectra Physics) that produces ~1-mJ pulses at 780 nm of ~120-fs duration at a 1 kHz repetition rate. About 80% of the fundamental light was used to pump an optical parametric amplifier (OPA) that generates tunable signal and idler beams in the infrared. Excitation pulses in the 470 to 500-nm range were generated by sum-frequency mixing of the signal beam from the OPA with the residual 780-nm fundamental light. Probe pulses in the 580 to 640-nm range were produced either by second harmonic generation of the OPA signal beam or by sum-frequency mixing of the idler beam from the OPA with the residual fundamental. The probe pulses were split into signal and reference beams that were detected with matched Si photodiodes and digitized on a shot-by-shot basis using a fast gated current-integrating analog-to-digital converter (LeCroy).

Time-resolved PL experiments were performed with the aid of an optically-triggered streak camera (Axis Photonique). The camera consists of a sensitive photocathode followed by ion focusing optics that accelerate the photoelectrons towards a phosphor screen. During the electrons' flight towards the phosphor screen, a linear voltage ramp is applied to a pair of deflection plates. The electrons that arrive first are thus deflected less than those that arrive later in time, so that when the electrons reach the phosphor screen they are spread out into a line, or streak. The light from the streak on the phosphor screen is recorded and digitized by a CCD camera, providing a signal that consists of amplitude (proportional to the number of electrons) as a function of CCD pixel position (proportional to the arrival time). The relation between the pixel position and time (~0.3 ps/pixel for the sweep rate used in most of our experiments) is determined by the slope of the voltage ramp applied to deflect the photoelectrons. We measured the pixel position/time conversion factor by scattering some of the excitation light into the camera and then changing the arrival time of the excitation pulse using an optical delay. This calibration also served to verify the linearity of the voltage ramp over the range of CCD pixels at which the PL signal was collected.

In principle, for collection of PL following a single laser shot, the time resolution of the streak camera should be equal to the temporal width of the excitation pulse. In practice, however, it is nearly impossible to measure streaks from a single laser shot at the excitation intensities we wish to explore, so averaging over multiple streaks is required. When averaging at a 1 kHz repetition rate, jitter between the arrival time of the excitation pulse and the start of the linear voltage ramp on different laser shots limits the time resolution of the averaged experiment. For the experiments reported here, triggering of the voltage ramp could be done in one of two ways. For experiments where a wide dynamic range in time ($\geq$ 200 ps) is required, the voltage

ramp was triggered electronically with a digital delay generator synchronized to the switch-out Pöckels cell of the regenerative amplifier. This provides a shot-to-shot jitter when averaging of ~50 ps, as seen in the PL traces in Fig. 1.[62] For higher-time resolution experiments, the voltage ramp was triggered optically by the arrival of the remaining 20% of the 780-nm fundamental laser pulses onto a pair of photoconductive switches. With optical triggering, the shot-to-shot jitter is limited only by the transit time of the carriers in the photoconductive switches, resulting in a time resolution of ~3 ps, but experiments in this mode are limited to times < 200 ps. Low-jitter optical triggering was used to collect all the PL data shown in this paper (except that in Fig. 1).

The key results of this paper are related to our ability to measure SE and PL dynamics under the same experimental conditions. In all the data presented below, SE and PL experiments were performed with identical sample excitation geometries, and at identical excitation intensities. To do this, the MEH-PPV film samples were placed at ~45° with respect to the propagation direction of the incoming excitation laser pulse. For SE experiments, the probe beam was detected in transmission, while PL was collected at 90° from the excitation beam using a 50-mm focal length camera lens. To avoid scatter, the SE probe beam was blocked during PL collection. To minimize deleterious effects from photo-oxidative damage, all of the experiments were performed (except where noted for the investigation of photodamaged samples) under dynamic vacuum in a 3-window optical cryostat. To further minimize potential damage, the samples were excited through the substrate,[7] and excitation intensities were kept lower than 10 $\mu J/cm^2$ at all times.[11,46]

Steady-state PL spectra also were obtained under identical excitation conditions as the time-resolved data by deflecting the emission that would have struck the streak camera cathode

into an optical fiber connected to a spectrophotometer (Ocean Optics). In both the SE and PL experiments, the relative polarization of the excitation and probe (or emitted) light were set at the magic angle, 54.7°, to avoid artifacts due to reorientation of the dipole of the emitting species. For experiments investigating only a limited spectral portion of the PL, absorptive glass filters (Schott) were placed in front of the streak camera photocathode; the filters were removed when collecting the spectrally-integrated PL. We emphasize that the width of the spectral sections measured is considerable, and may limit the precision of the spectrally-selected PL measurements because of non-uniformity in the spectral response of the streak camera's photocathode.

MEH-PPV was synthesized according to literature procedures,[65,66] and had an average molecular weight of 190,000 g/mol. All polymer processing, handling and characterization was performed either in the inert atmosphere of a nitrogen dry-box or under dynamic vacuum in the optical cryostat. The MEH-PPV films used for all the experiments were spin cast from chlorobenzene solution onto ITO-coated glass substrates. The ITO-coated substrates were chosen because the high refractive index of ITO prevents waveguiding of the PL in the film that leads to amplified spontaneous emission,[67] which could interfere with the dynamics being studied in the present experiments. A few experiments were performed on films that were intentionally photo-oxidized by simultaneous exposure to light and air. All the experiments were performed at room temperature.

III. Results and Discussion:

A. Comparing the PL and SE dynamics of MEH-PPV Films: To uncover the presence of interchain species in the ultrafast photophysics of MEH-PPV films, we begin by comparing the decay dynamics of selected spectral portions of the PL to pump-probe SE results collected using

a probe wavelength in the same region of the spectrum. Figure 3 outlines the spectral regions employed for the experiments: the thick solid curve shows the steady-state fluorescence spectrum of the MEH-PPV film and the dotted curves show the steady-state PL collected through selected optical color filters. We will refer to the portion of the filtered emission that has its intensity maximum near 580 nm as the "blue" PL, and the portion of the filtered emission that peaks near 640 nm as the "red" PL. The two dashed curves show the spectra of the two probe laser pulses used in the pump-probe SE experiments, centered around 580 and 640 nm, respectively.

Figure 4 compares the decay of the blue PL (solid diamonds) to the simultaneously collected 580-nm SE (open circles) at a relatively low excitation intensity (~400 nJ/cm^2); the two traces are normalized to the same value at the emission maximum. A direct comparison of the SE and PL data is not straightforward because of the large difference in time resolution of the two experimental techniques: the SE data is taken at ~0.3-ps time resolution, whereas the PL data suffers from the ~3-ps jitter of the optical trigger on the streak camera. Thus, to better compare the two sets of data, we have developed the following mathematical procedure: First, the SE signal was fit to a multiexponential function convoluted with a 0.3-ps Gaussian representing the pump-probe instrument response;[68] the fit is shown in Fig. 4 as the thin dotted line (which overlaps the open circles). Second, the analytical multiexponential function extracted from the fit was then numerically re-convoluted with a ~3-ps Gaussian that is characteristic of the streak camera instrumental response. The result of this reconvolution is shown in Figure 4 as the thin dashed curve (which overlaps the solid diamonds at times $\leq$ 3 ps); this curve represents the SE decay as it would have appeared if measured with the time resolution of the streak camera.

The decay of the blue PL in Figure 4 clearly does not match the reconvoluted 580-nm SE signal starting at times as early as 5 ps: the PL decays more quickly than the SE. At longer times, however, the two signals become parallel (not shown). This suggests that the PL signal monitors a fast (few-ps) photophysical event in the semiconducting polymer film that is invisible in the 580-nm-probe SE experiment, and that the two experiments monitor identical kinetics at longer times. We assign the early-time difference to energy migration, which we believe should be a much more important contribution to the PL signal than to the SE. This is because immediately after ultrafast laser excitation, the PL spectrum of MEH-PPV films has considerable amplitude at wavelengths bluer than the steady-state PL spectrum (i.e. significant amplitude to the blue of 550 nm; *cf.* Fig. 3).[41,42] This blue-shifted PL component, which is the emission from higher-energy excitons, decays in a few picoseconds as migration to lower-energy sites occurs via Förster energy transfer. The rapid PL decay observed in Figure 4 occurs on a time scale consistent with others' assignment of early-time energy migration.[18–21,41] The SE data in Figure 4 is not sensitive to this early-time energy transfer because it does not contain information about hot exciton emission to the blue of the steady-state spectrum, probing only the cooler exciton dynamics near 580 nm.

To further test this assignment of the fast blue PL decay from MEH-PPV films to early-time energy transfer, we collected a series of PL decay traces using long-pass optical filters to cut different portions of the bluest part of the collected emission. We found that as we removed the bluest part of the emission (not shown), the fast part of the blue PL decay became smaller in amplitude, approaching that of the reconvoluted SE as the spectrum of the collected PL approaches that of the 580-nm probe pulse. In other words, the data in Figures 2B and 4 show the limiting case where all the blue emission is collected, providing the most dramatic

contribution of energy migration to the PL decay. We performed similar experiments on MEH-PPV solutions and found an almost negligible dependence of the PL decay rate on the collection wavelength, verifying that the early-time decay of the PL signal in the film results from interchain energy transfer. We note that it was not possible to directly compare the PL and SE dynamics at the very blue edge of the emission spectrum because overlap of the probe pulse with the ground-state absorption of MEH-PPV led to contamination of the pump-probe signal with ground-state bleaching dynamics.

Figure 5 compares the pump-probe dynamics of MEH-PPV films monitored at 640 nm to the dynamics of the red portion of the PL (*cf.* Fig. 3) at both a low excitation intensity (panel A) and a high excitation intensity (panel B); as with Figure 4, the open circles show the pump-probe SE data, the solid diamonds show the time-resolved PL, and the dashed curves show the effective SE data at the streak camera's time resolution using the reconvolution procedure. Unlike the 580-nm pump-probe data in Figure 4, which begins decaying immediately after the instrument response, the low intensity 640-nm pump-probe data in Figure 5A, after an instrument-limited turn-on, continues to increase for a few picoseconds before beginning to decay. This rising feature of the emission is not evident in the red PL (or reconvoluted SE) dynamics because it takes place on a time scale faster than the instrument resolution of the streak camera. The most plausible origin of this fast rise component in the pump-probe data is energy migration. It makes sense that exciton migration from blue-emitting to red-emitting sites would produce a delayed appearance of emission on the red portion of the spectrum: this is the same process that produces the fast decay of the blue emission seen in Figures 2B and 4. Although this assignment makes sense, it is not immediately clear why the rise of the red PL is much less distinct than the corresponding disappearance of the blue PL. The fact that the rise of the red

emission is difficult to see also has been investigated via fluorescence upconversion by several groups, who concluded that the red PL signal consists of a superposition of a rising component from the migrating excitons plus a comparable decaying component caused by changes in the vibronic structure of the PL spectrum as the hot excitons cool.[18,19] It is also possible, as we will discuss in the next section, that E-EA has different effects at the blue and red portions of the spectrum, leading to an apparent enhancement of the fast decay of the blue PL.

In addition to the small rise in the SE, the red SE/PL data in Figure 5 show an even more significant difference from the blue SE/PL data in Figure 4: the 640-nm SE decays faster than the red PL, exactly the opposite of what was observed for the blue SE/PL. Moreover, Figure 5 shows that the difference between the red SE and PL grows larger with time, rather than becoming constant with time as was the case for the blue SE/PL. Since energy transfer does not play an important role in the emission dynamics at wavelengths this red at times longer than a few picoseconds, the difference in dynamics between the 640-nm SE and the red PL must arise from the presence of a non-emissive species that absorbs at 640 nm and has dynamics that are distinct from the excitons responsible for the PL. Since the PL and SE dynamics are identical for isolated MEH-PPV chains in solution at all wavelengths, the SE/PL difference observed in Fig. 5 for MEH-PPV films provides direct proof for the existence of an excited interchain species that has its PA in the emission region. Moreover, the fact that the difference between the SE and PL becomes more pronounced at higher excitation intensities (Figure 5B) suggests that the interchain species responsible for the PA in this region has intensity-dependent behavior, as we discuss in the next section.

B. Intensity-Dependent Photophysics and Exciton-Exciton Annihilation in MEH-PPV Films: We saw above in Figure 2A that the PL dynamics of MEH-PPV films are sensitive to the

excitation intensity due to the possibility that exciton-exciton annihilation can take place when the polymer chains are closely packed in the film environment. Since the data presented in Figures 4 and 5A were taken at low excitation intensities, we have confidence in our assignment that the fast emission decay at blue wavelengths and SE rise at red wavelengths are due largely (although not entirely) to energy migration. At higher excitation intensities, however, the photophysics of MEH-PPV films become more complex, exhibiting a combination of both energy migration and E-EA. This can be seen in Figure 6, which compares the PL dynamics for the same red and blue portions of the emission spectrum indicated in Figure 3 (and studied in Figures 4 and 5) at two excitation intensities that differ by a factor of ~20.

In the left panel of Figure 6, the dynamics of the blue PL at the two different intensities are shown normalized to the maximum of each signal. In the right panel of Figure 6, the corresponding red PL traces at both intensities are shown (with the time axis reversed) scaled to match their blue counterparts at a time long enough (~150 ps) that neither energy migration nor E-EA should play a significant role, so that only emission from thermalized intrachain excitons contributes to the signals. When normalized in this fashion, there is a clear difference in the heights of the red PL signals at time zero. This height difference indicates that the effects of E-EA are not uniform across the emission spectrum of MEH-PPV films: the fast initial decay at high excitation intensities is more pronounced on the blue side of the emission spectrum than on the red side of the emission spectrum. This suggests that E-EA is more efficient on the blue side of the spectrum: In other words, blue-emitting (hot) excitons that have not yet undergone Förster energy transfer have a faster rate of E-EA than red-emitting (thermalized) excitons produced by energy migration.[69] To the best of our knowledge this is the first experimental demonstration of

higher exciton-exciton annihilation efficiency for high-energy excitons, which indicates that hot excitons have a higher mobility than thermalized excitons.

The variation in the efficiency of E-EA with emission wavelength also explains the fact that different groups have measured bimolecular recombination coefficients for conjugated polymer films that differ by over an order of magnitude.[6–10,27,46] The bimolecular recombination coefficient (β) is obtained by fitting the experimental results to a non-linear differential equation that describes the time-dependent population density of emissive excitons:[70]

$$\frac{dN(t)}{dt} = -\frac{N(t)}{\tau} - \frac{\beta}{\sqrt{t}} N^2(t) \qquad (1)$$

where the only adjustable parameters are the intrachain exciton fluorescence lifetime (τ) and the bimolecular coefficient (β). The data for the different spectral regions in Figure 6 was fit to Eq. (1) using a global value for τ, but allowing β to vary between to the two sets of data. The bimolecular recombination coefficient that best fit the blue PL decay was found to be 60% higher than the best-fit β for the red region of the spectrum. The fact that E-EA is not uniform across the emission spectrum fits well with the conclusions of stimulated photoconductivity depletion experiments by Rothberg and co-workers, who found that hot excitons are more strongly correlated with the presence of charge carriers that give rise to photoconductivity than thermalized excitons.[38]

Finally, the enhancement of E-EA on the blue side of the spectrum may also be responsible for the fact that the amplitude of the fast blue PL decay does not precisely match the amplitude of the fast red PL rise, as mentioned above. In other words, the rapid decay of the blue PL (such as that seen in Figure 2B) observed by many groups may arise not just from energy migration but from a combination of energy migration and the enhanced E-EA of hot excitons.

The fact that E-EA is important to the photophysics of MEH-PPV films also allows us to understand the intensity dependence of the red SE and PL explored in Figure 5. The creation of the interchain species is reflected by the difference in the dynamics measured by these two experimental techniques. Figure 5 shows that not only is the difference between the red SE and PL at high excitation intensities larger in amplitude than the difference at lower intensities, but also that the SE/PL difference increases faster with time at higher excitation intensities; for example, the dashed line and solid diamonds start to diverge by ~7 ps in Fig. 5B, but not for ~20 ps in Fig. 5A). This suggests that the non-emissive interchain species responsible for the PA at this wavelength are created as a byproduct of E-EA: the number of interchain absorbing species grows non-linearly with increasing excitation intensity, as would be expected for a bi-molecular reaction. This idea of interchain species being created as a byproduct of E-EA is in line with the arguments published by McBranch and co-workers.[10–12]

We can learn more about the interchain species responsible for the PA by taking advantage of the fact that the lifetime of interchain species is typically much longer than that of the intrachain exciton. Thus, at some point following excitation, the long-lived interchain absorption component of the pump-probe signal will be larger than the stimulated emission component from the shorter-lived intrachain excitons, causing the pump-probe signal to change sign from negative (net SE gain) to positive (net transient absorption). Figure 7 shows the long-time portion of 640-nm pump-probe experiments on MEH-PPV films at three different excitation intensities; the three traces are normalized at time zero, as shown in the inset. Even for the scan at 0.7 $\mu J/cm^2$ (the same as in Figure 5A), the SE gain transforms into a net absorption at times longer than ~400 ps, indicating that even at the lowest pump intensity for which we can reliably measure SE, interchain species are present. In addition, Figure 7 shows that as the excitation

intensity is increased, the point at which the SE gains turns over to the net absorption shifts to progressively earlier times. Since E-EA should not affect the dynamics at times > 100 ps, this shift of the cross-over point confirms that the number of interchain species formed scales nonlinearly with excitation intensity.

C. Nature of the Absorbing Interchain Species in MEH-PPV Films: The results presented above, in conjunction with the ideas of McBranch and co-workers[10–12] and Denton et al.[7,8] suggest that interchain species can be formed as a byproduct of E-EA. This leads to the question of the nature of the interchain species formed by E-EA, and whether or not the interchain species are better described as a neutrally-delocalized excimer or a charge-separated polaron pair. To explore this question, we also performed a series of experiments on intentionally-oxidized MEH-PPV films. It is well known that the carbonyl groups along the polymer backbone that result from oxidative damage are good electron traps.[34,71] Thus, excitons that encounter carbonyl defects are readily split into charge-separated species, or polaron pairs, leading to a lower PL quantum yield. Fig. 8 shows the results of our intensity-dependent PL experiments on intentionally oxidized MEH-PPV films. As expected, the PL decay of the oxidized films was both faster and less sensitive to excitation intensity than the PL decay of pristine films.[34,46,71] Moreover, our pump-probe experiments on oxidized MEH-PPV films show a very early turn-over of the signal from SE gain to transient absorption: the turn-over occurrs at delay times ranging from 20 to 80 ps depending on the degree of sample oxidation and the intensity of the excitation pulse (also see, for example, Fig. 10 in Ref. 46). Since we know that the species responsible for the PA in the oxidized films are polarons, this result suggests that the interchain species created by E-EA in pristine samples, which show a similar behavior, are also associated with polarons, and thus, likely consist of polaron pairs. This fits well with the idea that in

pristine films, the Auger interaction between two excitons produces a doubly-excited exciton that has more than enough energy to dissociate, producing the same spectral signature as when dissociation is caused by interaction with a defect. This reasoning is also consistent with the observations of Heeger and co-workers, who have argued that at least 10% of the excitations at typical pump-probe excitation intensities produce the infrared absorptive signatures associated with polarons.[50,51]

Given that interchain polaron pairs are formed in conjugated polymer films at high excitation intensities as byproducts of E-EA or by the dissociation of doubly-excited intrachain excitons, the question remains as to whether or not polaron pairs or other types of interchain species are formed directly upon excitation, even at low intensities. Figure 7 shows that even at the lowest excitation intensities at which we could perform pump-probe experiments (sub-$\mu J/cm^2$),[72] the spectral signatures of an interchain PA with dynamics distinct from the emissive exciton are obvious. In addition, the results presented in Figure 7 show that the absorption offset at long times does not depend on intensity to the same degree as the initial decay of the SE signal. This suggests the presence of a directly-excited interchain species with a PA distinct from that of the interchain species produced by E-EA.

The idea that there can be more than one kind of interchain species in conjugated polymer films is consistent with previous work from our group where we used an NSOM-based solvatochromic technique to determine the dipole moment of the weakly-emitting interchain species in thermally-annealed MEH-PPV films. The results provided evidence for multiple interchain species with vastly different excited-state dipoles, ranging from near zero (consistent with excimers) to ~12-15 D (consistent with polaron pairs whose charges are separated by ~4 Å).[47] We also found evidence from NSOM-based third-harmonic generation experiments that

ground-state aggregates also exist in annealed MEH-PPV films.[48] This previous work, taken together with work from other groups[10,39,51] and with the results presented above, leads us to a picture of the interchain behavior of conjugated polymer films in which excimers and aggregates are the dominant interchain species at low excitation intensities, but polaron pairs dominate at higher excitation intensities or in films with significant numbers of exciton-dissociating defects.

Figure 9 tests the idea that there are multiple types of interchain excited states in films of conjugated polymers by comparing the results of two different pump-probe experiments at probe wavelengths that are very close in energy. The short-time pump-probe dynamics, presented in Figure 9A, show an initial fast decay at 600 nm that is absent at 640 nm. The difference looks similar to what might be expected at a single probe wavelength at two different excitation intensities. However, the spectrally-integrated PL dynamics monitored during each of the pump-probe scans (Figure 9B, inset) for the two experiments match perfectly, verifying that the two pump-probe scans were taken at the same excitation intensity. The two probe wavelengths are also spaced closely enough in energy that differences in the rate of energy migration or E-EA should be negligible. Thus, the faster pump-probe decay dynamics at 640 nm relative to 600 nm likely result either from changes in the vibronic structure of the emission during cooling[18,19] or from differences in the dynamics of the underlying interchain PA at the two probe wavelengths, or from a combination of both.

How can the interchain PA explain the wavelength-dependent pump-probe dynamics observed in Figure 9? The decay of the pump-probe signal at 600 nm is faster than that at 640 nm (Fig. 9A), but the 640-nm signal transforms into an absorption signal at an earlier delay time than the 600-nm signal (Fig. 9B). These two effects can be reconciled by arguing that the spectrum of the interchain PA undergoes a dynamic shift to the blue. We expect interchain

species, whether polaron pairs or excimers, to have their absorption maximum in the near IR,[10,32,33,46] to the red of the probe wavelengths investigated in Figure 9. Thus, the directly-excited interchain PA appears instrument-limited with little amplitude at 600 nm but a higher amplitude at 640 nm. As the interchain spectrum shifts to the blue, the amplitude of the PA rises faster at 600 nm than at 640 nm, explaining the apparently faster decay of the SE at 600 nm. Once the interchain PA has ceased shifting, however, its amplitude is still higher at 640 nm than 600 nm, explaining why the cross-over of the pump-probe signal to a net absorption occurs earlier at 640 nm than 600 nm.

The proposed blue-shift of the interchain PA might be the result of cooling if the interchain species is formed hot, or the blue shift might be indicative of the presence of multiple interchain species, which have different absorption spectra and appear at different rates. For example, if polaron pairs absorb to the blue of interchain excimers or aggregates, then the delayed appearance of polarons as the byproduct of E-EA would lead to a dynamic blue-shift of the interchain PA, which was initially due to directly-excited excimers or aggregates. Although these ideas are speculative, the different pump-probe dynamics observed in Figure 9 verify that even independent of morphology,[45,46] the photophysics of conjugated polymers are complex, characterized by a mixture of exciton emission, interchain absorption, energy migration, and wavelength dependent E-EA.

IV. Conclusions

In summary, we have simultaneously measured the SE and PL dynamics of MEH-PPV films as a function of excitation intensity and spectral position. We found that for low-intensity excitation, energy migration of hot intrachain excitons dominates the emission dynamics of the higher-energy portion of the PL spectrum at early times, whereas the low-energy portion of the

spectrum reflects the dynamics of thermalized excitons. At high excitation intensities, on the other hand, E-EA emerges as a process that causes exciton population decay at early times in competition with energy migration. Moreover, we found that E-EA occurs more efficiently for hot excitons, implying that hot excitons have a higher mobility than thermalized excitons. In addition, our comparison of SE and PL dynamics under the same excitation conditions clearly showed that non-emissive interchain species are created as a byproduct of E-EA. By performing similar experiments on intentionally oxidized samples, we assigned the interchain absorbing species produced by E-EA to polaron pairs. The results also suggest that the interchain PA undergoes a dynamic shift to the blue at early times. Finally, we believe that other kinds of interchain species, such as excimers and aggregates, are created directly upon excitation, even at low intensities.

In combination, the dependence on morphology and the complexity of the excited-state dynamics can lead to many pitfalls in interpreting the photophysics of conjugated polymer films. Photoexcitation of semiconducting polymer films can result in energy migration and thermalization of hot excitons, wavelength-dependent E-EA, and a dynamically shifting PA from different interchain species such as excimers, aggregates and polaron pairs. All of these processes have distinct photophysical signatures that heavily overlap in the spectral region where the polymer fluoresces. This implies that even with very detailed photophysical information of the type presented here, it is still quite difficult to extract quantitative information about the fate of the initial photoexcitation. In particular, our results suggest that interpretations based on experiments that use only a single probe wavelength can be misleading, explaining why so many groups have come to so many apparently contradictory conclusions concerning the fundamental nature of the photophysics of conjugated polymer films.

Acknowledgements: This work was supported by the National Science Foundation under grant number DMR-0305254, and by the donors of the Petroleum Research Fund of the American Chemical Society under grant number 37029-AC5,7. B.J.S. is a Cottrell Scholar of Research Corporation and a Camille Dreyfus Teacher-Scholar.

Figure Captions:

Figure 1: The excited-state emission dynamics of a dilute solution of MEH-PPV in chlorobenzene following excitation with ~100-fs light pulsee at 490 nm at two different excitation intensities. The emission dynamics are measured simultaneously in two different ways: via pump-probe stimulated emission (SE) using a 580-nm probe pulse (open symbols) and via spectrally-integrated photoluminescence (PL) using a streak camera (solid and dashed curves). The excitation intensities for each experiment are indicated in the legend.

Figure 2: Excited-state PL dynamics of an MEH-PPV film spin-cast from chlorobenzene onto an ITO-coated glass substrate measured using the streak camera: (A) The spectrally-integrated PL decay at a low excitation intensity (0.025 $\mu J/cm^2$, dotted curve), a medium excitation intensity (0.16 $\mu J/cm^2$) dashed curve) and a high excitation intensity (0.64 $\mu J/cm^2$, solid curve); the three curves are normalized to the same amplitude at $t = 0$. (B) Spectrally-selected portions of the PL spectrum at the same high intensity as in A; the two curves are normalized to the same maximum intensity at $t = 0$; see Figure 3 for the definitions of the "red" (dashed curve) and "blue" (solid curve) portions of the PL spectrum.

Figure 3: Steady-state PL spectrum of an MEH-PPV film cast from chlorobenzene (solid curve), and spectrally-selected portions of the PL spectrum using optical filters: the "red" portion of the PL (dark dotted curve) peaks at 640 nm, whereas the "blue"" portion of the PL (light dotted line) peaks at 580 nm. The spectra of the 580-nm (light dashed curve) and 640-nm (dark dashed curve) probe pulses used for the pump-probe SE experiments are also shown.

Figure 4: Comparison between the simultaneously-collected SE dynamics probing at 580 nm (open circles) and the "blue" PL dynamics (solid diamonds) for an MEH-PPV film cast from chlorobenzene excited at 490 nm collected simultaneously at a relatively low excitation intensity (0.4 $\mu J/cm^2$). The dotted curve is a multiexponential fit to the SE data, and the dashed line is the reconvolution of the fit with a ~3-ps Gaussian characteristic of the time resolution of the PL experiments; see text for details.[68]

Figure 5: Comparison between the simultaneously-collected SE dynamics probing at 640 nm (open circles) and the "red" PL dynamics (solid diamonds) for an MEH-PPV film cast from

chlorobenzene excited at 490 nm. Panel (A) shows the normalized comparison at a relatively low excitation intensity (0.7 μJ/cm^2), and panel (B) shows the comparison at a high excitation intensity (3 μJ/cm^2). In both panels, the dashed curves represent the SE data with the effective time resolution of the streak camera used to measure the PL; see text for details.[68]

Figure 6: Comparison of the "blue" and "red" PL dynamics at a low excitation intensity (0.05 μJ/cm^2, solid curves) and a high excitation intensity (1 μJ/cm^2, dashed curves) following excitation of an MEH-PPV film cast from chlorobenzene excited at 490 nm. Panel (A) shows the two "blue" PL decays, normalized to the same amplitude at t = 0; panel (B) shows the two "red" PL decays, normalized to the value of the "blue" PL decay at the same intensity at 150 ps (as shown more clearly by the reversed time axis), a time at which only singlet intrachain excitons are expected to contribute to the signals.

Figure 7: Comparison of pump-probe SE dynamics probing at 640 nm at three different excitation intensities for an MEH-PPV film cast from chlorobenzene excited at 490 nm. The three traces at a low intensity (0.7 μJ/cm^2, solid circles), a medium intensity (1.5 μJ/cm^2, open diamonds), and a high intensity (3.0 μJ/cm^2) are normalized to the same amplitude at $t = 0$. The main panel shows a magnification of the long-time part of the pump-probe data, while the inset shows the early-time portion. The dotted curves are fits to the data meant to guide the eye.

Figure 8: Comparison between the simultaneously-collected 580-nm SE (open symbols) and spectrally-integrated PL (solid curves) at two different excitation intensities for an intentionally-oxidized MEH-PPV film excited at 490 nm; the excitation intensities are indicated in the figure legend.

Figure 9: Comparison of the pump-probe SE dynamics at both 600 nm (open circles) and 640 nm (solid diamonds) for an MEH-PPV film cast from chlorobenzene excited at 490 nm. SE decay monitoring at 600 nm (open circles) and 640 nm (solid diamonds). Panel (A) shows the short-time dynamics, whereas panel (b) shows a magnification of the longer-time dynamics. The inset to panel (B) shows the simultaneously-collected PL dynamics for both experiments, verifying that the two SE experiments were performed at the same excitation intensity.

References:

[1] J. H. Burroughes, D. D. C. Bradley, A. R. Brown, R. N. Marks, K. Mackay, R. H. Friend, P. L. Burns and A. B. Holmes, Nature **347**, 539 (1990).

[2] D. Braun and A. J. Heeger, Appl. Phys. Lett. **58**, 1982 (1991).

[3] S. E. Shaheen, C. J. Brabec, N. S. Sariciftci, F. Padinger, T. Fromherz and J. C. Hummelen, Appl. Phys. Lett. **78**, 841 (2001).

[4] G. Yu, J. Gao, J. C. Hummelen, F. Wudl and A. J. Heeger, Science **270**, 1789 (1995).

[5] N. C. Greenham, I. D. W. Samuel, G. R. Hayes, R. T. Phillips, Y. A. R. R. Kessener, S. C. Moratti, A. B. Holmes and R. H. Friend, Chem. Phys. Lett. **241**, 89 (1995).

[6] R. G. Kepler, V. S. Valencia, S. J. Jabos and J. J. McNamara, Synth. Met. **78**, 227 (1996).

[7] G. J. Denton, N. Tessler, N. T. Harrison and R. H. Friend, Phys. Rev. Lett. **78**, 733 (1997).

[8] G. J. Denton, N. Tessler, M. A. Stevens and R. H. Friend, Synth. Met. **102**, 1008 (1999).

[9] M. Stevens, C. Silva, D. M. Russel and R. H. Friend, Phys. Rev. B 63, 165213 (2001).

[10] B. Kraabel, V. I. Klimov, R. Kohlman, S. Xu, H.-L. Wang and D. W. McBranch, Phys. Rev. B **61**, 8501 (2000).

[11] E. S. Maniloff, V. I. Klimov and D. W. McBranch Phys. Rev. B **56**, 1876 (1997).

[12] B. Kraabel, V. I. Klimov, R. Kohlman, S. Xu, H-L. Wang and D. W. McBranch, Phys. Rev. B **61**, 8501 (2000).

[13] J. Z. Zhang, M. A. Kreger, G. Klaener, M. Kreyenschmidt, R. D. Miller and J. C. Scott, Proc. SPIE **3145**, 363 (1997).

[14] S. A. Jenekhe and J. A. Osaheni, Science **265**, 765 (1994)

[15] I. D. W. Samuel, G. Rumbles and C. J. Collison, J. Phys. Chem. B **52**, R11753 (1995).

[16] I. D. W. Samuel, G. Rumbles, C. J. Collison, R. H. Friend, S. C. Moratti and A. B. Holmes, Synth. Met. **84**, 497 (1997).

[17] I. D. W. Samuel, G. Rumbles, C. J. Collison, S. C. Moratti and A. B. Holmes, Chem. Phys. **227**, 75 (1998).

[18] R. Kersting, B. Mollay, M. Rusch, J. Wenisch, G. Leising and H. F. Kauffmann, J. Chem. Phys. **106**, 2850 (1997).

[19] Ch. Warmuth, A. Tortschanoff, K. Brunner, B. Mollay and H. F. Kauffmann, J. Lumines. **76**, 498 (1998).

[20] R. F. Mahrt, T. Pauck, U. Lemmer, U. Siegner, M. Hopmeier, R. Hennig, H. Bassler, E. O. Gobel, P. Haring Bolivar, G. Wegmann, H. Kurz, U. Scherf and K. Mullen, Phys. Rev. B **54**, 1759 (1996).

[21] J. Sperling, F. Milota, A. Tortschanoff, C. Warmuth, B. Molky, H. Bassler and H. F. Kaufmann, J. Chem. Phys. **117**, 10877 (2002).

[22] U. Lemmer, S. Heun, R. F. Mahrt, U. Scherf, M. Hopmeier, U. Siegner, E. O. Gobel, K. Mullen and H. Bassler, Chem. Phys. Lett. **240**, 373 (1995).

[23] J. H. Hsu, W. S. Fann, P.-H. Tsao, K.-R. Chuang and S. A. Chen, J. Phys. Chem. A **103**, 2375 (1999).

[24] R. Chang, J. H. Hsu, W. S. Fann, J. Yu, S. H. Lin, Y. Z. Lee and S. A. Chen, Chem. Phys. Lett. **317**, 153 (2000).

[25] J. W. Blatchford, S. W. Jessen, L.-B. Lin, T. L. Gustafson, D.-K. Fu, H.-L. Wang, T. M. Swager, A. G. MacDiarmid and A. J. Epstein, Phys. Rev. B **54**, 9180 (1996)

[26]A. J. Epstein, J. W. Blatchford, Y. Z. Wang, D. D. Gebler, S. W. Jessen, L. B. Lin, T. L. Gustafson, D. K. Fu, H. L. Wang, T. M. Swager, and A. G. MacDiarmid, Synth. Met. **78**, 253 (1996)

[27] S.-H. Lim, T. G. Bjorklund and C. J. Bardeen, J. Chem. Phys. **118**, 4297 (2003).

[28] T. G. Bjorklund, S-H. Lim and C. J. Bardeen, Synth. Met. **126**, 295 (2002).

[29] T. G. Bjorklund, S.-H. Lim and C. J. Bardeen, J. Phys. Chem. B **105**, 11970 (2001).

[30] T.-Q. Nguyen and B. J. Schwartz J. Chem. Phys. **116,** 8198 (2002).

[31] T.-Q. Nguyen, R. Y. Yee and B. J. Schwartz, J. Photochem. Photobio. 144, 21 (2001).

[32] M. Yan, L. J. Rothberg, E. W. Kwock and T. M. Miller, Phys. Rev. Lett. **75**, 1992 (1995).

[33] J. W. P. Hsu, M. Yan, T. M. Jedju and L. J. Rothberg, Phys. Rev. B **49**, 712 (1994).

[34] L. J. Rothberg, M. Yan, F. Papadimitrakopoulos, M. E. Galvin, E. W. Kwock and T. M. Miller, Syn. Met. **80**, 41 (1996).

[35] P. Wang, C. J. Collison and L. J. Rothberg, J. Photochem. Photobio. A **144**, 63 (2001).

[36] C. J. Collison, L. J. Rothberg, V. Treemaneekarn and Y. Li, Macromol. **34**, 2346 (2001).

[37] P. Wang, C. M. Cuppoletti and L. J. Rothberg, Synt. Met. **137**, 1461 (2003).

[38] L. J. Rothberg, M. Yan, A. W. P. Fung, T. M. Jedju, E. W. W. Kwock and M. E. Galvin, Synth. Met. **84**, 537 (1997).

[39] R. Jakubiak, C. J. Collison, W. C. Wan, L. J. Rothberg and B. R. Hsieh, J. Phys. Chem. A **103**, 2394 (1999)

[40] R. Chang, J. H. Hsu, W. S. Fann, K. K. Liang, C. H. Chiang, M. Hayashi, J. Yu, S. H. Lin, E. C. Chang, K. R. Chuang, and S. A. Chen, Chem. Phys. Lett. **317**, 142 (2000).

[41] G. R. Hayes, I. D. W. Samuel and R. T. Phillips, Phys. Rev. B **52**, 11569 (1995).

[42] G. R. Hayes, I. D. W. Samuel and R. T. Phillips, Synth. Met. **84**, 889 (1997).

[43] M. Zheng, F. Bai and D. Zhu, J. Photochem. Photobio. A **116**, 143 (1998).

[44] T-Q. Nguyen, V. Doan and B. J. Schwartz, J. Chem. Phys. **110**, 4068 (1999).

[45] B. J. Schwartz, Ann. Rev. Phys. Chem. **54**, 141 (2003).

[46] T-Q. Nguyen, I. B. Martini, J. Liu and B. J. Schwartz, J. Phys. Chem. B **104**, 237 (2000).

[47] R. D. Schaller, L. F. Lee, J. C. Johnson, L. H. Haber, R. J. Saykally, J. Vieceli, I. Benjamin, T.-Q. Nguyen and B. J. Schwartz, J. Phys. Chem. B **106**, 9496 (2002)

[48] R. D. Schaller, P. T. Snee, J. C. Johnson, L. F. Lee, K. R. Wilson, L. H. Haber, R. J. Saykally, T.-Q. Nguyen and B. J. Schwartz, J. Chem. Phys. **117**, 6688 (2002).

[49] A. Dogariu, D. Vacar and A. Heeger, Phys. Rev. B **58**, 10218 (1998).

[50] D. Moses, A. Dogariu and A. J. Heeger, Chem. Phys. Lett. **316**, 356 (2000).

[51] P. B. Miranda and A. J. Heeger, Phys. Rev. B **6408**, 1201 (2001).

[52] D. Vacar, E. S. Maniloff, D. W. McBranch and A. J. Heeger Phys. Rev. B **56**, 4573 (1997).

[53] E. M. Conwell, Phys. Rev. B 57, 14200 (1998).

[54] J. Yu, D. H. Hu and P. F. Barbara, Science, **289**, 1327 (2000).

[55] T. Huser and M. Yan, J. Photochem. Photobio. A **144**, 43 (2001).

[56] C. W. Hollars, S. M. Lane and T. Huser, Chem. Phys. Lett. **370**, 393 (2003).

[57] T.-Q. Nguyen, R. C. Kwong, M. E. Thompson and B. J. Schwartz Appl. Phys. Lett. **76**, 2454 (2000)

[58] J. M. Lupton, I. D. W. Samuel, R. Beavington, P. L. Burn and H. Bassler, Adv. Mat. **13**, 258 (2001).

[59] F. Hide, M. Diaz Garcia, B. J. Schwartz, M. Andersson, Q. Pei and A. Heeger Science **273**, 1833 (1996).

[60] X. Long, M. Grell, A. Malinowski and D. D. C. Bradley, Opt. Mater. **9**, 70 (1998).

[61] S. V. Frolov, Z. V. Vardeny and K. Yoshino, Phys. Rev. B **57**, 9141 (1998).

[62] In order to collect the entire population decay, the PL traces in Fig. 1 were measured at ~50-ps time resolution. Higher-time resolution PL data shows that the early-time PL dynamics also matches perfectly with the early-time SE dynamics.

[63] T.-Q. Nguyen, J. Wu, V. Doan, B. J. Schwartz and S. H. Tolbert, Science **288**, 652 (2000).

[64] B. J. Schwartz, T.-Q. Nguyen, J. Wu and S. H. Tolbert, Synth. Met. **116**, 35 (2001).

[65] F. Wudl, P. M. Alleman, G. Srdanov, Z. Ni and D. McBranch, ACS Symp. Ser. **455** (1991).

[66] F. Wudl and S. Hoger, PCT Patent Application 1991, WO 94/20589.

[67] F. Hide, B. J. Schwartz, M. A. Díaz-García and A. J. Heeger, Synth. Met. **91**, 35 (1997).

[68] We typically used 2 or 3 exponentials to fit the SE data. We note that we do not attribute any physical significance to the multiexponential form chosen to fit the SE data: the fits simply provide an empirical means to reproduce the data for the sole purpose of reducing the noise in the reconvolution step.

[69] Throughout this paper, we refer to "hot" excitons as those localized on shorter (higher-energy) conjugated segments, characterized by blue PL. In contrast, we refer to "thermalized" excitons as those localized on longer (lower-energy) conjugated segments, characterized by a redder PL.

[70] The $1/\sqrt{t}$ factor can be derived in two different ways, either assuming that the excitons do not diffuse to annihilate each other but that the spatial distribution of excitons changes because the closest pairs get depopulated first, or assuming that exciton diffusion is confined to only one dimension along the polymer backbone. See, S. L. Dexheimer, in *Optical Properties of Fullerenes and Fullerene-based Materials,* J. Shinar, Z. V. Vardeny and Z. H. Kafafi, eds. (Dekker, New York, 2000) as well as reference 52.

[71] M. Yan, L. J. Rothberg, F. Papadimitrakopoulos, M. E. Galvin and T. M. Miller, Phys. Rev. Lett. **73**, 744 (1994).

[72] We were able to obtain PL decay traces at even lower intensities (down to fractions of a nJ/cm^2), but found that the PL dynamics remain intensity-dependent even at the lowest intensities we could measure; this suggests that non-linear processes still contribute significantly to the photophysics even in our "low-intensity" scans.

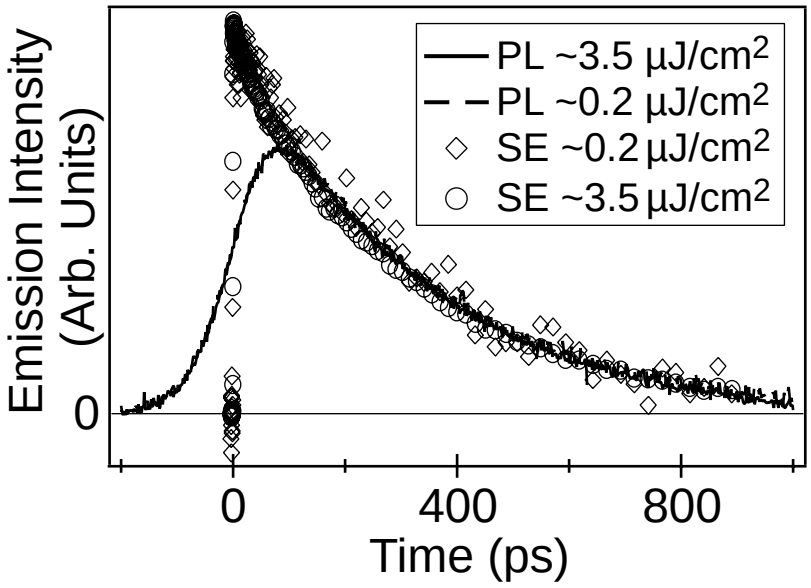

Figure 1:Martini et al.

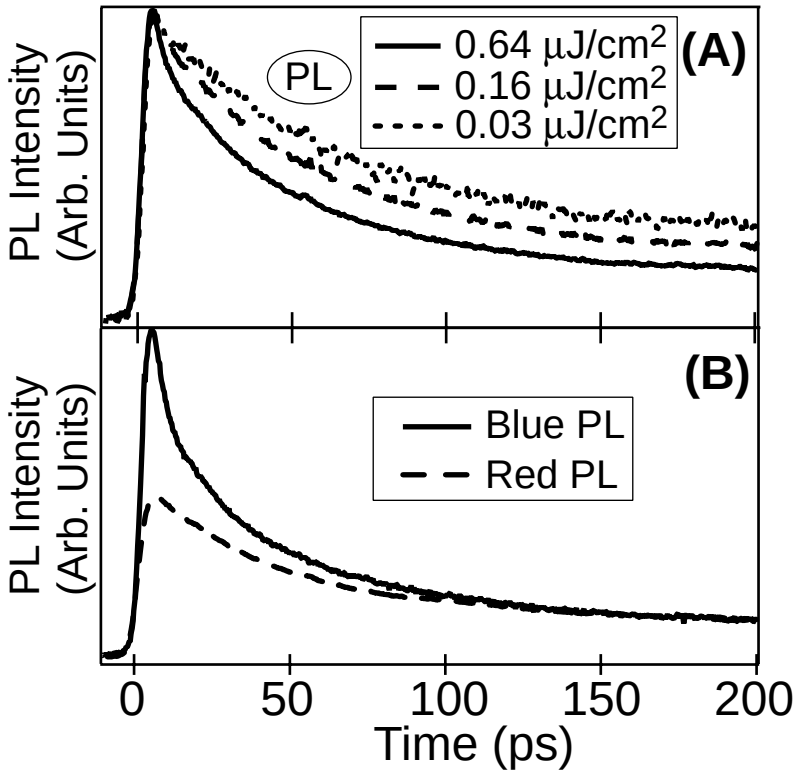

Figure 2: Martini et. al

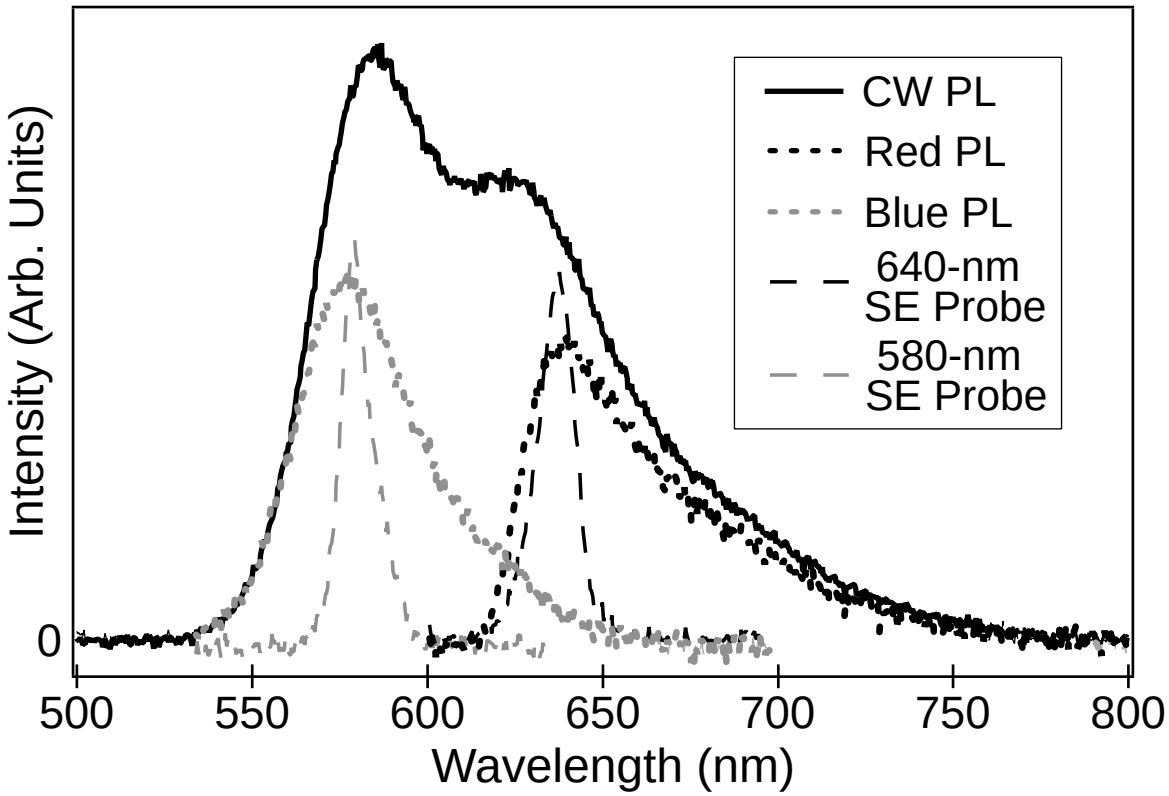

Figure 3: Martini et al

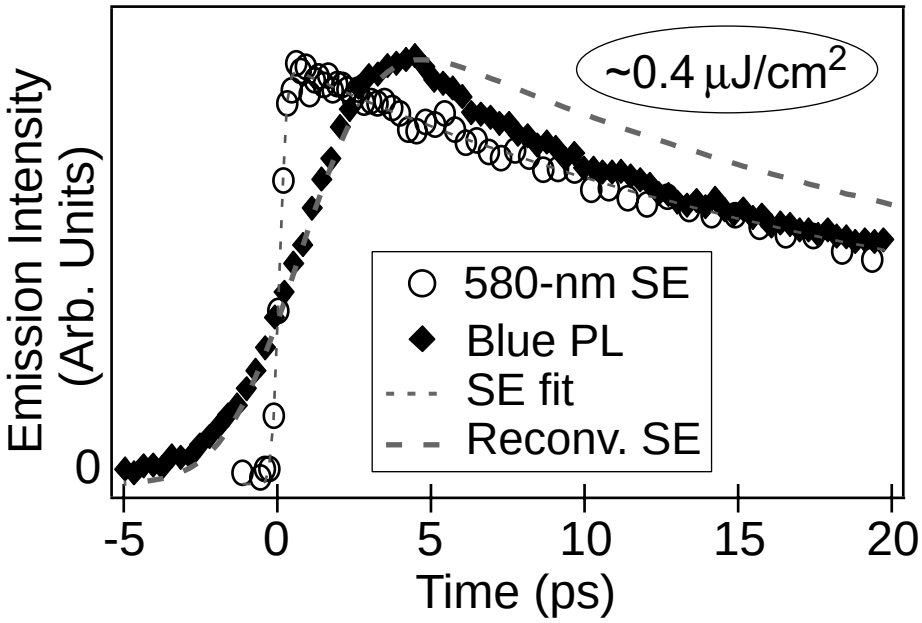

Figure 4: Martini et al

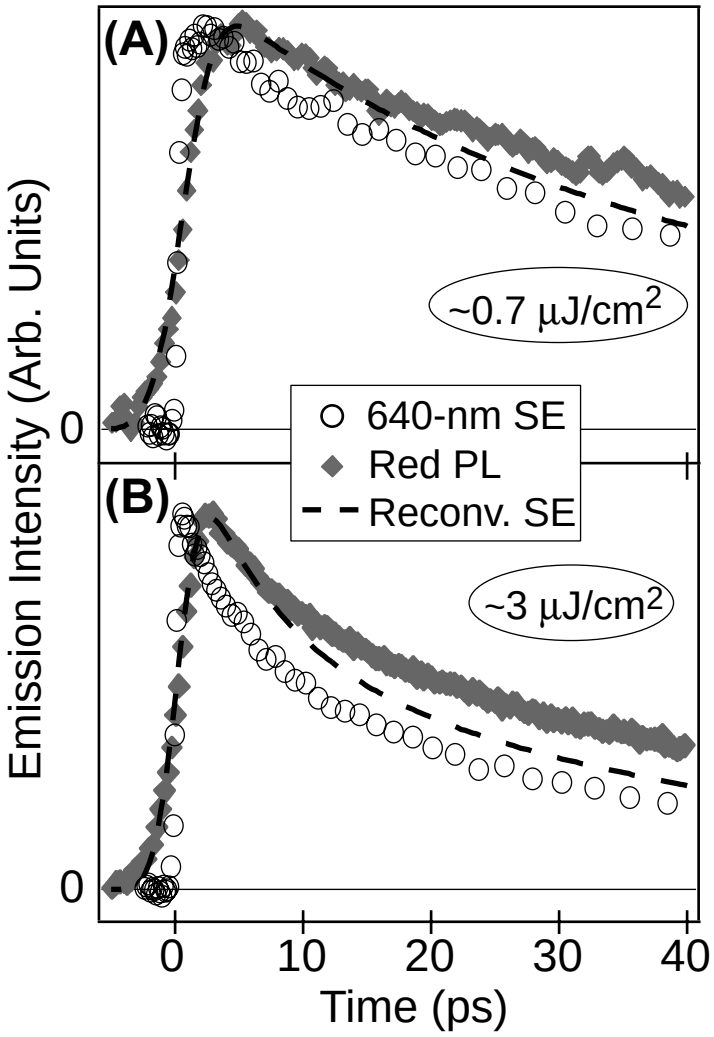

Figure 5: Martini et al

Figure 6: Martini et al

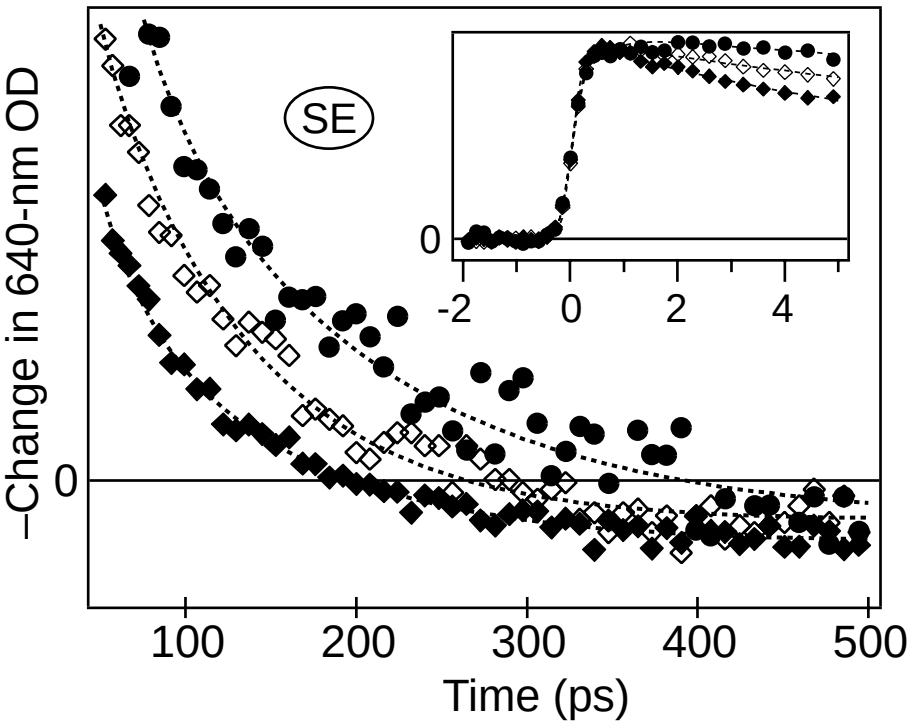

Figure 7: Martini et al.

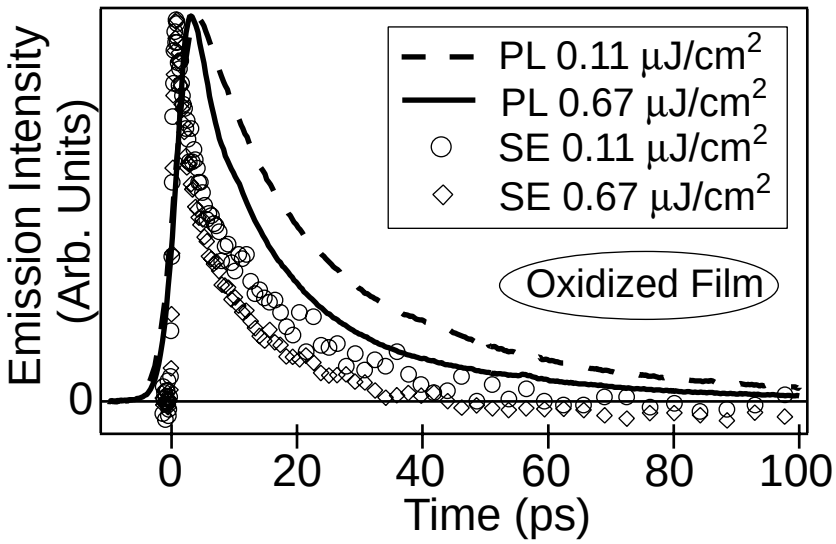

Figure 8: Martini et al.

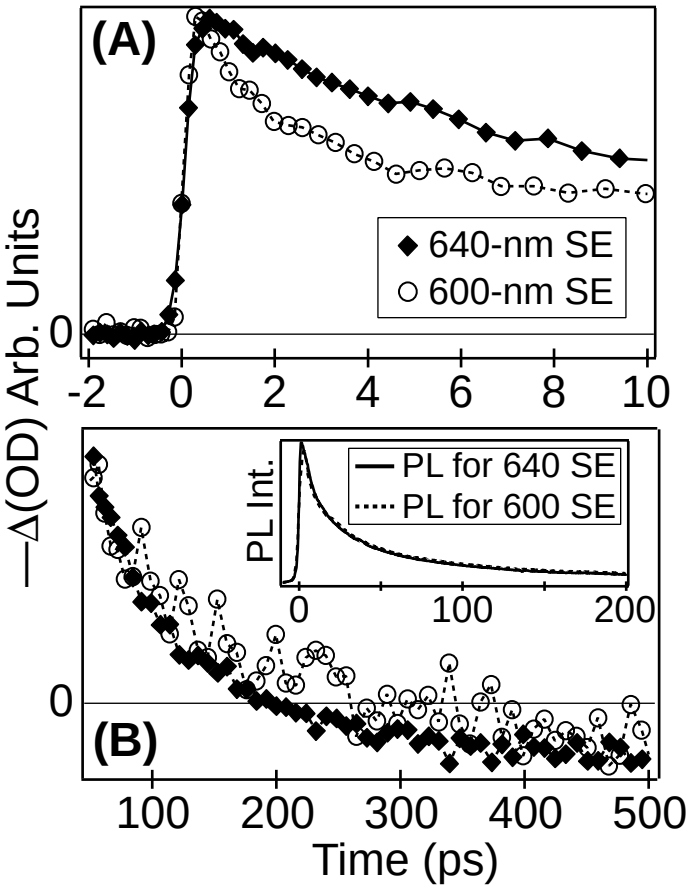

Figure 9: Martini et al